

Stability of the Cyclotron Resonance Scattering Feature in Her X-1 with RXTE

D. E. Gruber, W. A. Heindl, R. E. Rothschild, W. Coburn

Center for Astrophysics & Space Sciences, University of California, San Diego 92093

R. Staubert, I. Kreykenbohm, and J. Wilms

Institut für Astronomie und Astrophysik, Abt. Astronomie, Universität Tübingen, D-72076

Tübingen, Germany

Received _____; accepted _____

ABSTRACT

Five observations of the hard X-ray spectrum of Her X-1 from *RXTE* show that the ~ 41 keV energy of the cyclotron scattering line is constant within statistics of a few percent per observation. The overall spectral shape, on the other hand, varies somewhat, with an RMS of 2%. If the 41 keV feature truly originates as cyclotron resonance scattering in an unchanging 3×10^{12} Gauss dipole field not far above the neutron star surface, these observations constrain the average height of scattering to within a range of 180 meters. This is consistent with models which put the radiating structure within meters of the surface of the neutron star. In other pulsars observed line centroid changes have been correlated with luminosity changes, and if interpreted as variations of the height at which scattering takes place, many hundreds of meters are required. These *RXTE* data, which sample nearly a factor of two in unabsorbed luminosity, are in conflict with a particular model for such an extended radiating structure. Comparison with other observations over many years indicates strongly that the centroid energy of this absorption line has increased some time between 1991 and 1993 by 23%, from 34 keV to 41 keV. Moreover, the cutoff energy of the spectral continuum increased at the same time from 16 keV to 20 keV, which is, within the statistical error of 5%, in direct proportion to the centroid. This may be a sign that both these characteristics of the spectrum are controlled in the same way by the magnetic field strength in the region of scattering.

Subject headings: pulsars:individual(Her X-1) — X-rays:stars

1. Introduction

The accreting X-ray pulsar, Hercules X-1, emits a spectrum with a localized depression at roughly 40 keV which is generally interpreted as an absorption line resulting from scattering of photons on electrons whose motions are constrained in one spatial dimension to transitions between Landau levels in a teraGauss magnetic field at the neutron star’s polar cap. Commonly referred to as a cyclotron line, this feature was discovered in 1977 (Trümper et al. 1978), although first identified phenomenologically as an emission feature at somewhat higher energy. This feature in Her X-1 has since been observed repeatedly (e.g. Gruber et al. 1980, Voges 1984, Tueller et al. 1984, Soong et al. 1988, Mihara 1995, Kunz 1995, Dal Fiume et al. 1998). Similar features have also been identified in the hard X-ray spectra of many of the accreting X-ray pulsars (e.g. Mihara 1995, Heindl et al. 1999, Dal Fiume et al. 2000). Cyclotron lines afford a diagnostic of plasmas under extreme conditions and can provide a key to the structure of the magnetosphere and the mass flow.

Mihara et al. (1998) have reported a study of repeated observations with *Ginga* of cyclotron lines in a number of X-ray pulsars. In a few instances, although not with Her X-1, they found a correlation with X-ray luminosity which was consistent with the cyclotron scattering taking place from hundreds to many hundreds of meters above the neutron star surface, at the peak of an “accretion mound” structure proposed by Burnard, Arons & Klein (BAK, 1991). BAK predict a strong dependence of this height on accretion flow. Thus in this model variability of the cyclotron line energy can also be an important diagnostic of the scattering region and accretion process.

Studies of line formation (Mészáros & Nagel 1985, Isenberg, Lamb & Wang 1998, Araya-Gochez & Harding 2000) have indicated the possibility of line profiles which deviate from the simple Gaussian and Lorentzian profiles which have been used for analysis to date. Such deviations are evident as particularly broad lines (Heindl 1999, Orlandini 1999).

However, the line of Her X-1 is narrower, and measurement of structure beyond the first and second moments (centroid and width) requires detector resolution higher than the $\delta E/E$ of a few obtainable with inorganic scintillators, as well as very large collecting area and observing time.

Using data from five observations over two years with the large-area instruments aboard Rossi X-Ray Timing Explorer (*RXTE*) we have performed detailed spectroscopy of the spectral continuum, the cyclotron line and the fluorescent iron line of Her X-1. We find only minor variability between these observations. Exercising careful data selection, we have compared the results with those from earlier measurements between 1977 and 1994. For this purpose the *HEAO-1* data were freshly analyzed with modern software and spectral models. To a level of perhaps 10% the pre-1991 spectral shapes are consistent with each other, as are the spectra from 1994 onwards. Between 1991 and 1994 there strongly appears to have been a change of the cyclotron line centroid and the cutoff energy of the continuum. This is in marked contrast to the power law index and exponential fold energy, for which the average values remained constant to within a few percent. In §2 we describe instrumentation and observations, in §3 analysis and results, and in §4 we briefly discuss possible interpretations. Preliminary results from a portion of this *RXTE* data set have been reported earlier (Gruber et al. 1997, 1998, 1999).

2. Instruments and Observations

The *RXTE*, launched late in 1995 into low earth orbit, performs pointed observations with the Proportional Counter Array (PCA, Jahoda et al. 1996) and the High Energy X-Ray Timing Experiment (HEXTE, Rothschild et al. 1998). The PCA consists of five Xenon proportional counters (called PCU's) sensitive in the energy range 2–60 keV with 1400 cm² each. The HEXTE consists of eight NaI scintillator detectors of area 200 cm² each

and energy range 15–250 keV. Both instruments are non-imaging and have coaligned fields of view collimated to 1° FWHM. Time resolution was microseconds. Energy resolution was 16% at 6 keV for PCA, and 15% at 60 keV for HEXTE.

The five *RXTE* observations (Table 1) each consisted of several satellite orbits, each orbit typically containing 3300 seconds on-source. All five PCU’s were used except for the observations of 1996 August, for which only four detectors were operated. After the first observation one of the eight HEXTE detectors was lost for spectroscopic purposes. The observations were collected over two years from 1996 and 1997. Each was selected to be near the peak of the Her X-1 “main-on” state and to avoid periods of eclipse and other forms of obscuration, such as pre-eclipse dips. Exposures were varied, but averaged 15000 s per observation.

The study of long-term changes relies particularly on archival *HEAO-1* A-4 (Matteson 1978) data, which we re-analyzed with modern software and spectral models. The two Low-Energy Detectors of this experiment each had area 103 cm^2 and spectral resolution 25% at 60 keV. The A-4 instrument was quite accurately calibrated. The calibration is described in part in Jung (1986) and Gruber et al. (1989), and additional relevant details are given in the Appendix.

3. Analysis and Results

The spectral form characteristic (White, Swank & Holt 1982) of accreting X-ray pulsars, a power law of photon number index Γ , $E^{-\Gamma}$, and with high-energy exponential rolloff E_f above a cutoff energy E_c , $e^{-(E-E_c)/E_f}$, was the starting point for analysis. To represent cyclotron absorption we employed the multiplicative profile

$$e^{(-\tau \cdot \exp(-(E-E_r)^2/2\sigma^2))},$$

where E_r is the centroid, σ is the line RMS, and τ is the optical depth. Earlier work in the literature began with additive and subtractive forms to represent line emission. With the general acceptance of the line formation process as resonance cyclotron scattering of photons from the continuum, multiplicative profiles were adopted. With *Ginga* and *BeppoSAX* a nearly Lorentzian profile was also employed:

$$e^{(-\tau \cdot (\sigma \cdot E / E_r) / ((E - E_r)^2 + \sigma^2))},$$

with τ , E_r and σ as above. We report detailed results only with the Gaussian profile in optical depth, but note that best-fit values for the line centroid differ only by -5% using the Lorentzian profile, and a similar amount for subtractive profiles. All results of this analysis are significant also if the Lorentzian profile is used in place of the Gaussian. We note that the employment of any of these profiles is largely historical and heuristic. Recent calculations (Araya-Gochez & Harding 2000) indicate a wide variety of possible line profiles.

Spectra averaged over pulse phase were employed for this work. A major goal was comparison with historical observations, many of which are available only in this form. Although spectra can be strongly phase dependent in some pulsars, with Her X-1 only modest changes with phase have been observed for selected parameters, in particular the power law index change of 30% (Pravdo et al. 1977) and a 20% change of the cyclotron line centroid (Gruber et al. 1980, Voges 1984). Pulse phase-resolved spectroscopy will be reported in a later publication. The observations were collected at various orbital phases (Table 1), but we expect no effect from this, because a lack of spectral changes with orbit was reported by Pravdo (1976). Moreover, the eight *HEAO-1* observations of Soong et al. (1990) showed no orbital variation. We performed spectral analysis with the cut-off power law continuum model already mentioned, and we tried and rejected another model in current use, the Fermi-Dirac (Tanaka 1986). These forms are used empirically only: we are unaware of any theoretical forms for the spectral continuum which permit meaningful

comparison with the observed spectra.

3.1. *RXTE* Spectral Analysis

Data were selected from the five observations such that the source was unclipped either by the primary or the earth and such that characteristic absorption events (“dips”, $N_H > 10^{21} \text{cm}^{-2}$) were absent. A substantial dead-time correction was applied to the HEXTE data. The HEXTE background was directly measured by switching the HEXTE look direction on- and off-source every 16 seconds, while the PCA internal background was estimated with the *RXTE* software tool PCABACKEST and the strong-source background model. This model is known to have an accuracy of the order of a few percent. Following established procedure (e.g. Wilms et al. 1999) we tuned the background estimate to the observed high-energy portion of the data by adjusting a scaling factor to produce zero PCA net counts above 60 keV. The RMS correction for the five observations was 4.4%. As a further measure to limit sensitivity to residual background subtraction errors, PCA data below 3.5 keV and above 25 keV were not used, except as a check. Within the 3.5 – 25 keV range the average source spectrum was at least four times background, and usually much greater. Even with this favorable signal-to-background residuals to fits initially showed structure at the 1% level. We found very similar structure in power-law fits to the Crab spectrum with PCA, and we attributed this to imperfectly modeled background at the level of accuracy of the background model, about one milliCrab. We were able to model the spectrum of the extra background in the Crab observations as an extremely broad, $\sigma = 2.5$ keV, Gaussian line centered at about 5 keV. We then applied it successfully to remove the dominant residuals in the fits to Her X-1, and the adjusted constant of normalization again yielded a flux of close to one milliCrab, as with the Crab itself. Except for this extra background component and for details, our procedure for dealing with these systematic

errors closely follows that described by Wilms et al. (1999, see Appendix B). As a practical matter, the HEXTE data above 25 keV are statistically much stronger than the PCA, and very little statistical weight is gained by adding PCA data above 25 keV. As a check, however, we have performed joint fits including PCA data to 60 keV. The higher-energy PCA data are quite consistent with the HEXTE data. In particular, in each observation the PCA independently confirms the presence of the absorption line at about 40 keV. The HEXTE data range extended from 20 keV, chosen to be above the electronic threshold for all observations, to 100 keV, above which energy data were discarded because the Her X-1 signal was below detectability.

Standard PCA energy response matrices produced with version 5.0 ftools were employed. These were checked against contemporary Crab observations, and non-statistical errors of 0.25% RMS were thus measured. This error was applied to each PCA energy channel as a systematic error. This 0.25% error represents a refinement of the calibration procedures which earlier led Heindl et al. (1999) to assign a 1% systematic error. The residuals to the Her X-1 fits with this high-energy cutoff model for the continuum showed a depression at the cut energy. This was identified as an artifact of this spectral model, which has discontinuous slope at the cut energy. This artifact was quite effectively suppressed by modeling a Gaussian absorption at the cut energy with optical depth 0.15 and sigma 2.5 keV. We note that Burderi et al. (2000), in analyzing *BeppoSAX* data for Cen X-3, also found the need to introduce an empirical rounding function at the cutoff energy with this continuum. They used a polynomial rather than a Gaussian form.

With this model and the very low 0.25% systematic error for PCA, fits to all five observations produced acceptable chi-squares and a flat and featureless pattern of residuals. In particular, we found no evidence for the 18 keV spectral break reported from a *BeppoSAX* observation (Dal Fiume et al. 1998).

Fits to a power law with the Fermi-Dirac (Tanaka 1986) cutoff function,

$$(1 + e^{(E-E_c)/E_f})^{-1},$$

also with fold and cutoff energies but with continuous derivative, were tried in the hope of modeling the spectral turnover more simply. Instead, a pattern of correlated residuals over the entire PCA energy range resulted, strongly indicating a poor fit and functional mismatch with the data. This test with an alternative continuum did show, however, that best-fit values for the line centroid were even more insensitive to the choice of continuum than their 5% sensitivity to choice of line profile.

In Figure 1 we show the best fit and residuals for observation 2, which had the longest duration. The middle panel shows the large residuals, particularly at 40 keV, of a fit without cyclotron line, while the lowest panel shows the acceptable fit when the line is included. The displayed PCA data include the 0.25% systematic error per datum.

In Table 2 we list best-fit parameters and errors from the five observations for the successful continuum model with power law and high-energy cutoff, plus iron K emission and cyclotron scattering feature. In the last column of Table 2 are shown results of a simultaneous fit to all five observations with free normalizations for each but with the same spectral shape parameters, including line depth. For the fit to the combined data the large χ_r^2 of ~ 4.6 is dominated by small but real spectral changes from observation to observation, primarily in the spectral index and cutoff energy. We estimate the spectrum-to-spectrum variability to be 1.8% RMS.

Best-fit parameter values in Table 2 were determined by minimizing the χ^2 statistic, using the systematic plus statistical errors for PCA spectral data and statistical errors only for HEXTE. The parameter error estimates were determined from a number of Monte-Carlo realizations using xspec: starting with a best-fit model we determined the average and RMS scatter for each parameter. For the parameters which define the continuum shape these

experimentally-determined errors averaged a factor 1.8 greater than the values reported directly by *xspec*, while corresponding estimates for the parameters of the scattering line were larger only by a factor 1.1. These estimates are smaller than those obtained by the prescription of Lampton, Margon & Bowyer (LMB, 1976), which gave factors averaging 2.2 larger than the direct *xspec* estimates.

Given the satisfactory results obtained with the best-fit spectral model, we could also search for variability of the individual parameters of this model. For the five measured values of each parameter in Table 2 we calculated averages and chi-squares. With either our Monte-Carlo estimates or the LMB errors large chi-squares for the parameters for the continuum shape strongly indicated very significant but nevertheless modest variability. Conversely, for the scattering line parameters both methods indicated stability, with reduced chi-squares near unity or below. Reduced chi-squares using the LMB estimates for the three line parameter errors were all about 0.25, indicating ($P=0.001$) that the LMB errors are overestimated.

The parameters which depend most strongly on the correction for PCA systematic error are the power law index and the iron line parameters. The cutoff, fold and cyclotron line parameters are determined largely by the HEXTE data, for which pure statistical errors were employed.

Of special interest is the possible variability of the cyclotron line centroid. The five *RXTE* centroid values are consistent with no variability. The chi-square of 5.7 (4 dof) for the centroid values permits an extra random variability as high as 1.5 keV (90% confidence) in the centroid energy.

The five *RXTE* observations were each made in the first few days of a Her X-1 35-day main-on state. Strictly speaking, then, the measured 1.8% spectral stability applies only to the early part of the main-on. The spectrum varies somewhat with pulse phase (Soong et

al. 1990) and the pulsation shape is known to vary regularly with 35-day phase (Scott et al. 1997). So there is reason to expect spectral variability with 35-day phase. However, the *HEAO-1* observations (Soong et al. 1990), which sampled the main-on state fairly well, showed no change of pulse phase-average spectral shape with 35-day phase.

The contemporary observation with *BeppoSAX* (Dal Fiume et al. 1998), which has similar statistical weight to the *RXTE* observations, yielded similar results. The *BeppoSAX* values for the cyclotron line parameters agree with the *RXTE* values to within the errors of Table 2. There is reasonable agreement for the iron line parameters. The continuum parameters are harder to compare because of the 18 keV break in the *BeppoSAX* power law index, which we do not confirm. In the next section we compare these results with observations made well before the launch of *RXTE*. This comparison indicates significant changes for the cyclotron line energy and the cutoff energy of the continuum. Significant change was not found in other parameters of the spectrum.

The 41 keV absorption line was observed at high significance in all five *RXTE* observations. Trümper et al. (1978), interpreting the cyclotron feature as emission at 55 keV, reported a possible harmonic overtone, although this has never been confirmed. Multiple harmonic lines have been observed in the spectrum of a few other x-ray pulsars, most notably 4U0115+63 (Heindl et al. 1999; Santangelo et al. 1999), which has four or five. We have searched for a harmonic overtone of the 41 keV scattering feature by means of a simultaneous fit to the HEXTE data of all five observations. The resulting best-fit optical depth for the overtone at 82 keV is zero, and the 95% confidence upper limit is 0.23. This limit shows that the cyclotron scattering is quite different in Her X-1 than in 4U0115+63, whose overtones have optical depths greater than unity.

3.2. Reanalysis of *HEAO-1*

To permit more reliable comparison with earlier work we have re-analyzed archival *HEAO-1* A2 and A4 spectra using the same high-energy cutoff and line profile functions employed here with *RXTE* data. Another important reason for re-analysis is that considerable work (see Appendix) has gone into the calibration of the *HEAO-1* A4 since the results of Soong et al. (1990). For two of the *HEAO-1* observations we were able to fit simultaneously 1–18 keV data from an Argon counter of the A2 experiment (Rothschild et al. 1978), thereby obtaining a good measure of the power law index. One such fit is shown in Figure 2. Two sets of residuals are shown in Figure 2: the middle panel contains residuals to a fit without the cyclotron line and clearly shows a pronounced deficit at 35 keV; the bottom panel contains acceptable residuals to a fit which includes the line.

The *HEAO-1* spectral parameter values and errors shown in Table 3 are from this re-analysis. By comparison with Soong et al. (1990), values differ somewhat. The spectral index and cutoff energy are smaller by 20%, the fold energy is 10% larger, the line centroid (3% smaller) is nearly the same, and the line width is smaller by 30%. The change of line width is probably not significant, given the resolution and statistics. As with the *RXTE* data, we tested the sensitivity of the cyclotron line centroid value to different line profiles, as well as the two continuum models. We found changes only of the order of 1 keV, even less than with *RXTE*. Errors were estimated as described here for *RXTE*. They are a factor of 2-3 larger than those reported by Soong et al. (1990), who used a simpler procedure to estimate errors.

The most interesting result from the reanalysis are the *HEAO-1* values for the cutoff, which lie between 16 and 17 keV, considerably smaller than the 24 keV reported as a best-fit for *HEAO-1* on-pulse minus off-pulse spectra by Gruber et al. (1980), and also less than the 21 keV assumed by Soong et al. (1990). These two authors did not have the use of

the *HEAO-1* A2 data, which powerfully constrains the value of the spectral index. Indeed, the values of the spectral index, cutoff and fold are very highly correlated in the A4 data, because these data have a lower threshold at 13 keV. The correlation has the sense that overestimating the cutoff energy requires the fit to compensate by moving the index to a larger value and the fold energy to a smaller value. When we fit to the A4 data alone, the index moved to a value above unity, the cutoff energy moved to 18 keV, and the fold energy to 13 keV. A cutoff energy at 21 keV, as used by Soong et al. (1990), requires a chi-square higher than this A4-only best-fit by ~ 4 . Such a difference is reasonably consistent with small changes in the response matrix, background subtraction, and functional forms from those used earlier. We thus believe that the earlier cutoff values of Gruber et al. (1980) and Soong et al. (1990) were considerably overestimated, largely due to the limited spectral range of the A4 data. We note that the *HEAO-1* A2/A4 data sets are very well matched to the *RXTE* PCA/HEXTE data sets in spectral range and statistical significance. Therefore comparisons of spectral parameters between observations performed with these missions is much more reliable than between other pairs of missions.

3.3. Long Term Changes

The values for the line centroid in the present work are roughly consistent with measurements of values near 44 keV obtained between 1993 and 1995 with *CGRO*/BATSE (Freeman et. al 1996). The *RXTE*, *BeppoSAX* and BATSE values differ from all earlier measurements, which centered near 35 keV (Kunz 1995). Earlier data with good statistics and reliable energy calibrations include those from the *HEAO-1* A4 experiment (Soong 1988), the GRIS germanium detector (Tueller et al. 1984), the HEXE experiment aboard the Russian platform *MIR* (Kunz 1995), and *Ginga* (Mihara 1995). However, functional forms for the representation of the continuum and line profile have been various, making

comparison somewhat uncertain. In Table 3 we have collected reported results for continuum (power law with a high energy exponential cut off) and cyclotron line parameters. The iron line parameters, which did not change sensibly, are ignored.

The cyclotron energy between 1976 and 1996 is charted in Figure 3. Clearly, the data before 1991 are consistent with an average value near 35 keV and the data after 1991 are consistent with a higher average of 41 keV. When we analyze the parameters in Table 3 for the formal significance of a change of average value (a step function in time) using the F-test, we obtain the average values and significances shown in Table 4. The large reduced chi-squares are perhaps inevitable given calibration errors and somewhat differing functional forms for fits, as well as the possibility of variability on any time scale. Formal statistical results based on such high chi-squares are not valid. However the F-statistic, which is based here on the comparison of chi-squares for the null hypothesis of no change, χ_n^2 , and for a change between 1991 and 1994, χ_f^2 , should be more robust and provide at least an upper limit to the the null hypothesis (no change) probability. With this statistic the line centroid has in fact a very low significance $\leq 1.8 \times 10^{-11}$ for no change. Probably significant is a change of the cutoff energy, with $P_{null} \leq 0.01$. Possibly significant at 90% confidence are small changes of the power law index and fold energy, and a doubling of the scattering line width. If the Lorentzian line profile is substituted in the analysis, the changes are slightly less significant.

The observations of continuum cutoff energy relied almost entirely on the *HEAO-1* and *RXTE* measurements. The cutoff energy could not be measured with the many balloon experiments shown in Table 3 and Figure 3 because of atmospheric absorption below 25 keV. The MIR/HEXE experiment had an electronic threshold at 25 keV and was therefore insensitive to cutoff energy. The *BeppoSAX* fit was made with a more complicated continuum model with two inflection points near 20 keV, so could not be used. Finally,

errors were not stated for the *Ginga* observation. The most striking feature of the behavior of the cutoff energy is its apparent close proportionality to the centroid energy, shown in Figure 4. The dashed line displays proportionality with the best-fit factor of 2.03. The correlation coefficient for these data is 0.97, with a null (no correlation) probability of only $1.1 \cdot 10^{-6}$.

We conclude that a historical change has occurred in the values of at least two characteristics of the Her X-1 spectrum: the cyclotron scattering energy and the spectral cutoff energy of the power-law continuum.

4. Discussion

Models for the overall X-ray spectra and pulse shape from X-ray pulsars (Kirk et al. 1986; Mészáros & Nagel 1985) have had only moderate success in predicting the observed continuum spectral shapes. We concentrate therefore on the interpretation of the cyclotron line, especially in its bearing on the pulsar magnetic field. We discuss also the correlation of the continuum cutoff with centroid. The absence of sizeable change in the other spectral parameters should perhaps not be surprising given the likelihood that an important controlling factor in the spectral shape is the rate of energy release, and that this varied only over a factor of two in the joint *RXTE* and *HEAO-1* data sets, for which we can speak most authoritatively. The stability of the parameters of the fluorescent iron emission at 6.5 keV and their similarity to the values obtained with OSO-8 (Becker et al. 1977) and *BeppoSAX* (Dal Fiume et al. 1998) indicate that the geometry of the reprocessing site, usually thought to be at the magnetopause (e.g. McCray et al. 1982), has not changed dramatically.

4.1. Cyclotron Line Centroid Variability with the *RXTE* Dataset

The absorption feature is widely regarded to result from resonance scattering of electrons in a magnetic field (Trümper et al. 1978) of intensity $\sim 3 \times 10^{12}$ Gauss (Voges et al. 1982), given the earlier measurements of 35 keV for the centroid. These five *RXTE* observations give a new average value of 3.6×10^{12} Gauss and can be used to set limits to the range of magnetic field strengths sampled. These *RXTE* data are consistent with no variability of line centroid to within 3% RMS. The field strength at the scattering site is therefore also stable to a precision of 3%. The magnetic moment can be determined from the inferred field strength, to be 1.8×10^{30} Gauss-cm³, assuming magnetic dipole structure, scattering at the polar surface of the neutron star and a 10 km radius. For scattering somewhere above the surface, this limit constrains the range for the average height of scattering to within 180 meters (90% confidence) in a dipole field, and requires a somewhat higher magnetic moment.

Next, we test the *RXTE* data against a more specific process. There seems to be no general agreement on the structure of the radiating region of the polar cap of an X-ray pulsar. If a shock forms in the flow above the pole BAK (1991) predict an accretion mound of sizeable extent. Other theorists, however, most recently Bulik et al. (1995), place the site of deceleration of the accretion flow at the base of the neutron star atmosphere, with a scale height of less than a meter. The present results are consistent with the latter scenario, but they do not constrain the accretion mound scenario unless this is hundreds of meters or more in height. However, we note that if the observed line width of 5 keV or 12% is due largely to a mix of magnetic field strengths in a dipole field, then the scattering occurs over a range of the order of 1 km in height.

BAK estimate an accretion mound height of 650 meters for Her X-1, with a direct proportionality of this height to mass transfer rate (luminosity). Although BAK state that

the radiation escapes from the mound at its base, Mihara et al. (1999) have had some success modeling centroid variability in several pulsars with intensity under the assumption that the scattering occurs at the top of the mound. Mihara et al. (1999) do not find such a clear pattern, however, for Her X-1. As shown in Figure 5, the present *RXTE* data also rule out the BAK/Mihara centroid-intensity variability, to better than 3σ confidence. The *RXTE* observations span a 2–30 keV flux range of $(4.5\text{--}8)\times 10^{-9}$ erg-cm⁻²-s⁻¹, for which BAK/Mihara predict a change of 7 keV. In addition, there is no evidence in any of the *RXTE* observations for photoelectric absorption, therefore an actual correlation could not have been disguised by unrelated obscuration of the X-ray emitting region.

The fairly tight *RXTE* constraints on variability of line centroid, interpreted as a limit on the range for height of scattering in a dipole magnetic field, give some preference for emission at the stellar surface. We note, however, that on the pulsation time scale the change of line centroid with pulse phase reported by Soong et al. (1990) could be produced in the BAK/Mihara picture if the average height of scattering changes with viewing angle, i.e., pulse phase. It has not yet been decided observationally, however, whether it is the centroid that changes more with pulse phase or the line profile more generally.

4.2. Variability on long Time Scales

This new observation of a long-term change of cutoff energy closely proportional to the change of scattering energy suggests a common factor in producing both spectral features. This controlling factor, undoubted in the case of the scattering feature, is almost certainly the magnetic field strength. In a study of twelve X-ray pulsars with cyclotron lines Makishima et al. (1999) demonstrated a convincing correlation between the cutoff energy of the continuum and the line centroid. Their functional relation is a power law with index 1.4, thus $\text{cutoff} \sim \text{centroid}^{1.4}$. Could this population characteristic also apply

to changes in time with a single pulsar, as in this case? We find (Figure 4) that a power law relation with index 1.4 fits the *RXTE* and *HEAO-1* data much worse than simple proportionality. However, we note that the data in Figure 4a of Makishima et al. (1999) seem reasonably consistent also with direct proportionality, so that there may indeed be some correspondence.

These long-term spectral changes could result from a change of the height of scattering, although we can note that in this case the BAK/Mihara scenario would require *HEAO-1* fluxes two to three times what was observed, and thus can be ruled out.

Brown & Bildsten (1998) have reconsidered the structure of the settling mound addressed earlier by BAK and have developed a model with a more compact structure, of the order of 100 meters in height. In calculating the hydrostatic pressure of the accreted settling matter in this structure, they obtain a pressure comparable to the magnetic pressure, which distorts and spreads the magnetic field lines, thus lowering the magnetic field intensity. They give no time scale for significant change of this structure. The observed limit of 5 years to the period of change may be applicable to their model.

Ruderman et al. (1998) have a model of neutron stars in which motions of superfluid neutron vortices may alter the magnetic field in the core, which can result in movements of the stellar crust which in turn alter the surface magnetic field. The observed change of line centroid could thus in principle be related to a change of magnetic field in response to a change of structure. A structural change, in turn, would very likely produce a timing event. However, it is not known whether such a crustal change could produce a timing glitch large enough to be seen in the presence of accretion timing noise.

5. Conclusions

We have shown convincing evidence for a 23% historical change in the cyclotron line energy in the spectrum of Her X-1 through comparison of *RXTE* observations with earlier observations. For this purpose archival *HEAO-1* spectra were re-analyzed, using modern tools and spectral forms for consistency. On the other hand, the five *RXTE* observations, which span about two years, show no change, with a limit of about three percent. We also demonstrate a historical change of continuum cutoff energy which is closely proportional to the cyclotron centroid energy. This is the first good evidence to connect the cutoff energy, which is common to accreting pulsars, to the magnetic field. These *RXTE* data do not support a particular accretion mound scenario.

6. Acknowledgements

This work was supported in part by NASA under contracts NAS8–27974, NAS5-30720 and grant NAGW–449. The authors at Tübingen gratefully acknowledge support from German grants DLR 50 00 9605 and DAAD/Staubert. Valuable comments from the referee led to a much improved treatment and presentation.

Appendix: Calibration of the *HEAO-1* A4 LED detectors

The two Low Energy Detectors (LED's) of the High-Energy X-ray and Low-Energy Gamma-Ray Experiment (A4) aboard *HEAO-1* were thin NaI scintillators of area 103 cm² each, energy range 12–180 keV, and energy resolution 25% FWHM at 60 keV. Many spectral results were published from these detectors, but only a very brief description of the energy calibration and monitoring procedures has been reported (Jung 1986). For energy calibration the LED detectors were provided with ²⁴¹Am calibration sources whose events were recognized through a special pulse shape. But this calibration required special operating modes that were employed infrequently. Moreover, unexpected changes in the crystal optical interfaces following launch left the absolute energy calibration with these sources uncertain. Therefore an alternative procedure was devised which relied on the correct identification as well as monitoring of spectral lines in the instrument internal background. This background resulted largely from radioactive daughter isotopes produced by spallation interactions of cosmic rays and geomagnetically-trapped protons with the iodine nuclei in the detector. Most daughters are unstable and beta decay, producing a continuum in energy within the detector. But an alternative channel for positron decay is capture by the nucleus of an atomic electron in the K shell. This K-capture produces characteristic radiation whose total energy results from the fluorescent radiation of the electron cloud as it reconfigures as well as the nuclear deexcitation gamma ray, if any. A number of such lines were identified in the LED detectors (Gruber et al. 1988). The most useful line for calibration and monitoring was from ¹²⁵I (half life 60 days), for which there was a gamma with energy 35 keV and a total of 32 keV from the electronic cascade. Because all the charge was collected by the electronics in less than the several microsecond pulse shaping time, the summed pulse corresponding to 67 keV energy loss was observed. The identification of this isotope and line in the A4 data was quite secure, because the 60-day buildup of the activity at the beginning of the mission was clearly observed.

The most important complication for energy calibration for the A4 detectors was the energy-dependent efficiency of light production by the inorganic phosphor (Adams & Dams 1970). Light production in the crystal lattice is stimulated by fast electrons resulting from the photon interaction. This process apparently has a maximum efficiency at electron energy of 10–20 keV (e.g. Zerby, Meyer & Murray 1961). This variation in light output with energy for a HEXTE detector is shown in Figure 4 of Wayne et al. (1998). The energy-dependent efficiency was carefully calibrated prior to launch of the *HEAO-1* using radioactive sources. This calibration curve was then used to calculate the light production for a ^{125}I decay, whose energy is shared among several electrons ranging from a few keV to tens of keV. The light production was calculated to be equivalent to light originating from a single photon of 62.7 keV, not 67 keV. Use of the former number successfully resolved a problem in the interpretation of LED spectra: a strong spurious 40 keV emission line which appeared in the spectra of the Crab, Cyg X-1, and the diffuse X-ray background! Reassignment of the calibration energy from 67 keV to 62.7 keV completely removed this artifact in all these spectra. From the sensitivity to this feature alone we estimate the absolute accuracy of the A4 LED calibration as 2%. Other aspects of the calibration were discussed most fully in several UCSD PhD dissertations: effective area, Nolan (1982); angular response, Knight (1981); gain variability, monitoring and correction, Jung (1986).

REFERENCES

- Adams, F. and Dams, R., 1970, "Applied Gamma-Ray Spectrometry", (Oxford:Pergamon), pp 55-57.
- Araya-Gochez, R. A., & Harding, A. K., 2000, *Ap. J.*, 544, 1067.
- Becker, R. H. et al., 1977, *Ap. J.*, 214, 879.
- Brown, E. F. and Bildsten, L., 1998, *Ap. J.*, 496, 915.
- Bulik, T. et al., 1995, *Ap. J.*, 444, 405.
- Burderi, L. et al., 2000, *Ap. J.*, 530, 429.
- Burnard, D. Arons, J., and Klein, R., 1991, *Ap. J.*, 367, 575
- Dal Fiume, D. et al., 1998, *A&A*, 329, L41.
- Freeman, P. E. et al., 1996, in "Proceedings of the 3rd Huntsville Symposium", eds Kouveliotou, Briggs & Fishman, (New York:AIP), p. 172.
- Gruber, D. E. et al., 1980, *ApJ*, 240, L127.
- Gruber, D. E., et al., 1989, in "High-Energy Radiation Background in Space" eds. Rester & Trombka, (New York:AIP), p 232.
- Gruber, D. E., et al., 1997, in "Proceedings of the 4th Compton Symposium", eds Dermer, Strickland and Kurfess (New York:AIP), p. 744.
- Gruber, D. E., et al., 1998, in "The Active X-Ray Sky" eds Scarsi, Bradt and Giommi (Amsterdam:Elsevier), p 174.
- Gruber, D. E., et al., 1999, in "Proceedings of the 2nd Integral Workshop", in press.

- Heindl, W., et al., 1999, ApJ, 521, L49.
- Isenberg, M., Lamb, D. Q., and Wang, J. C. L., 1998, ApJ, 505, 688.
- Jahoda, K., et al., 1996, Proc. SPIE, 2828, 59.
- Jung, G. V., 1986, unpublished dissertation, UCSD.
- Kirk, J. G., 1986, A&A 169, 259.
- Knight, F. K., 1981, unpublished dissertation, UCSD.
- Kunz, M., unpublished dissertation, 1995, Univ. Tübingen.
- Lampton, M., Margon, B., & Bowyer, S., 1976, Ap. J., 208, 177.
- Makishima, K., et al., 1999, Ap. J., 525, 978.
- McCray, R., et al., 1982, Ap. J., 262, 301.
- Mészáros, P., and Nagel, W., 1985, Ap. J., 299, 138.
- Mihara, T., 1995, unpublished dissertation, University of Tokyo.
- Mihara, T., et al., 1998, Adv. Space Res., 22, 7, 987.
- Nolan, P. L., 1982, unpublished dissertation, UCSD.
- Orlandini, M. et al., 1999, Proceedings of 1999 Bologna Meeting, in press.
- Pravdo, S. H., 1976, unpublished dissertation, University of Maryland.
- Pravdo, S. H., et al., 1977, ApJ, 216,L23.
- Pravdo, S. H., et al., 1979, M. N. R. A. S., 188, 5.
- Rothschild, R. E., et al., 1978, Space Sci. Instr., 4, 265.

- Rothschild, R. E., et al., 1998, ApJ, 496, 538.
- Ruderman, M., et al., 1998, ApJ, 492, 267.
- Santangelo, A., et al., 1999, ApJ, 523, L85.
- Scott, D. M., et al., 1997, in “Proceedings of the Fourth Compton Symposium, eds Dermer, Strickland and Kurfess (New York, AIP), 748.
- Soong, Y., 1988, unpublished dissertation, 1998, University of California, San Diego.
- Soong, Y., et al., 1990, Ap. J., 348, 641.
- Tanaka, Y., 1986, in IAU Colloq. 89, eds D. Mihalas and K. H. Winkler, (New York, Springer), 198.
- Trümper, J., et al., 1978, Ap. J. (Letters), 219, L105.
- Tueller, J., et al., 1984, Ap. J., 279, 177.
- Voges, W., 1984, unpublished dissertation, LMU München.
- Voges. W., et al., 1982, Ap. J., 263, 803.
- Wayne. L., et al., 1998, Nucl, Inst & Meth. in Physics Res., Sect A, 411, 351.
- White, N. E., Swank, J. H., and Holt, S. S., 1983, Ap. J., 270, 711.
- Wilms. J., et al., 1999, Ap. J., 522, 460.
- Zerby, C. D., Meyer, A. & Murray, R. B., 1961, Nucl. Inst. Meth. 12, 115.

Fig. 1.— (Top panel) Fit with high-energy cutoff continuum and Gaussian absorptive line profile to PCA and HEXTE data from 1996 July in units of detector counting rate versus energy. Except above 70 keV, where adjacent channels have been grouped for display, original detector energy channels are shown. These oversample the actual detector energy resolution by factors of three to eight. (Middle panel) Residuals to fit *without* absorption line, showing strong and correlated deviations, particularly at 40 keV, the line energy. (Bottom panel) Residuals, now acceptable, to fit which includes the absorption line. PCA errors include a 0.25% systematic error, which dominates the statistical errors. HEXTE markings, x for Cluster A and o for cluster B, have been omitted in the top panel for clarity. Error bars are one sigma.

Fig. 2.— Spectral fit and residuals to *HEAO-1* data of 1978 Feb 24. The three panels are as in Figure 1. The 1-16 keV data are from an Argon-filled detector of the A2 experiment, and the 12-100 keV data marked with circles and crosses are from the two Low Energy Detectors of the A4 experiment. Errors (one sigma) are purely statistical. Original energy channels are shown, and these oversample the detector resolution by factors of two to four. Other than a negative feature at 4.5 keV, the fit is acceptable. The best-fit cyclotron energy is 33.2 keV and the cutoff energy 15.9 keV.

Fig. 3.— History of centroid energy of absorption line. Errors are one sigma, as estimated by the original investigators or in this paper for *RXTE* and *HEAO-1*. A pronounced change is evident following the *Ginga* measurement in 1990. Dashed lines indicate the averages for the earlier and later data. A similar and proportional change of the cutoff energy is also quite significant. The internal consistency of the *RXTE* data indicates that the errors have not been underestimated. Observations are listed by date and experiment in Table 3.

Fig. 4.— The value of the centroid energy of the cyclotron scattering versus the cutoff energy of the spectral continuum, with $1\text{-}\sigma$ errors. Correlation is formally highly significant, and

the dashed line shows the best-fit proportionality with constant 2.03. Errors are determined from the 68% joint confidence regions. A power law dependence with index 1.4 (dot-dashed line), as was observed in a population study by Makishima et al. (1999), fits quite a bit worse.

Fig. 5.— Measured line centroids versus 20-60 keV flux obtained with HEXTE-only datasets, with $1\text{-}\sigma$ errors. The line shows expected dependence predicted by Mihara (1999) from the model of BAK (1991), in which the mean luminosity corresponds to a height of 1 km above the polar cap for the scattering. The predicted dependence is not confirmed.

Table 1: Outline of Observations

Observation	Date	Duration in sec	Binary Phase Range [†]
1	1996 Feb	5000	.17-.23
2	1996 July	28000	.63-.93, .12-.46
3	1996 Oct	5800	.06-.08, .49-.52
4	1997 Sept	20000	.13-.38
5	1997 Nov	18000	.21-.40, .68-.74

[†] Zero phase is mid-eclipse, or superior conjunction

Table 2: Results of Spectral Fitting, PCA <25 keV plus HEXTE Data

date	1996 Feb	1996 July	1996 Oct	1997 Sept	1997 Nov	all
2-30 keV flux, units 10^{-9} keV cm^{-2} sec^{-1}						
flux	7.84	7.27	5.33	6.83	4.44	-
power law with high-energy cut-off continuum						
index [†]	0.855(4) [‡]	.862(4)	.841(5)	.901(4)	0.852(4)	.841(2)
cutoff	19.83(11)	20.23(8)	19.10(12)	20.27(9)	19.50(10)	19.60(9)
fold	10.87(22)	10.65(15)	10.02(19)	10.49(19)	10.08(16)	10.79(9)
Fe line						
eqw	.154(19)	.190(18)	.219(24)	.140(16)	.188(23)	.171(9)
centroid	6.625(31)	6.518(24)	6.524(25)	6.490(31)	6.393(33)	6.535(15)
sigma	.31(4)	.37(3)	.34(3)	.30(4)	.48(4)	.36(2)
scat. line						
depth	0.80(5)	0.74(3)	0.63(3)	0.66(5)	.67(4)	.75(2)
centroid	40.9(5)	40.8(3)	39.4(7)	40.1(4)	40.0(6)	41.0(2)
sigma	4.5(5)	4.9(3)	3.8(7)	4.7(4)	3.7(6)	4.9(2)
χ_r^2	1.10	0.99	0.94	0.98	1.08	4.56

[†] parameters have units keV except for index and depth, both dimensionless.

[‡] 68% statistical errors in parentheses apply to the last significant figure(s)

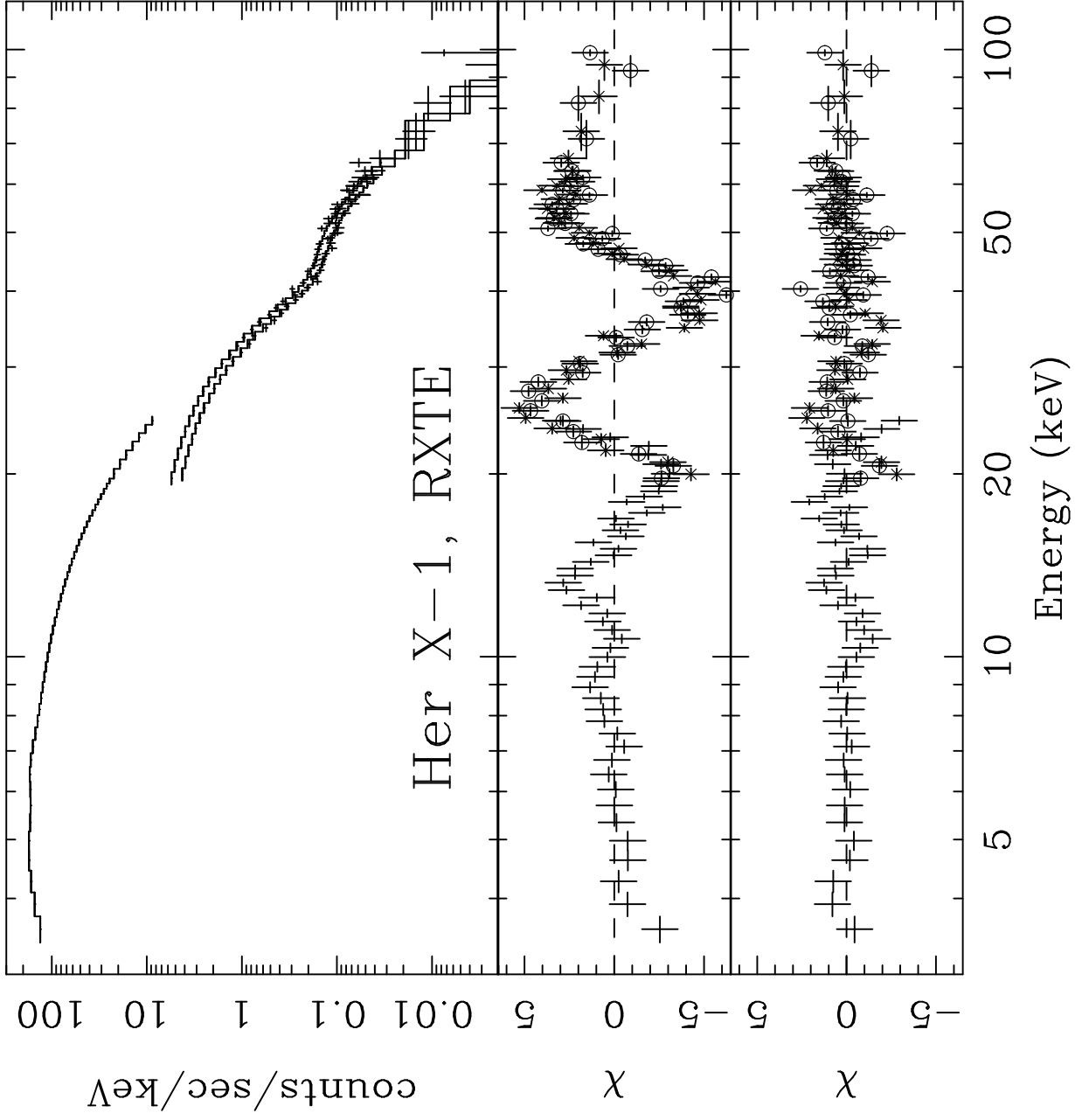
Table 3: Historical Observations of Parameters for Cut-off Continuum

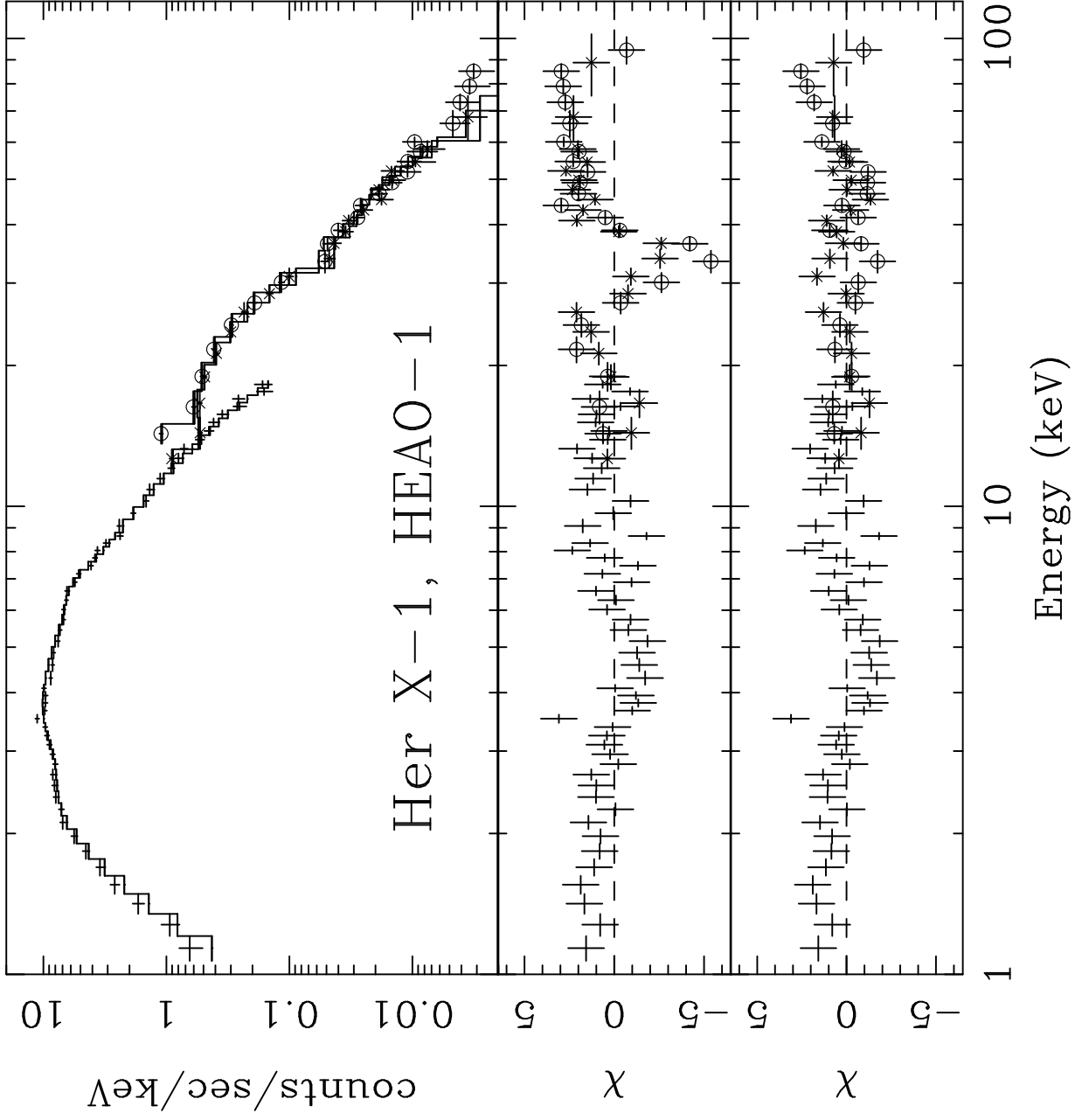
year	Data Set	Γ	E_c	E_f	τ	E_r	σ
+1900			keV	keV		keV	keV
77.671	BalloonHEXE			12.2(9)	3.2(6) [†]	36.8(14)	1.3
78.151	<i>HEAO-1</i>		16.4(9)	10.8(4)	1.20(55)	34.0(8)	2.9(13)
78.161	<i>HEAO-1</i>		16.6(10)	11.1(5)	1.48(98)	33.9(8)	2.5(14)
78.164	<i>HEAO-1</i>		16.1(15)	11.7(7)	1.78(81)	34.5(9)	3.4(13)
78.622	<i>HEAO-1</i>	.943(14)	16.0(4)	10.9(4)	1.16(37)	33.2(9)	2.6(13)
78.630	<i>HEAO-1</i>	.912(12)	16.8(4)	11.4(4)	0.87(9)	34.6(9)	4.5(11)
78.638	<i>HEAO-1</i>		16.9(5)	9.8(4)	0.68(17)	33.2(9)	
80.726	GRIS			9.9(16)		35.4(21)	3.59(188)
87.528	HEXE			10.6(10)	3.0(18)	33.8(18)	
87.618	HEXE			9.9(10)	1.6(10)	32.3(23)	
88.565	HEXE			10.8(20)	4.5(34)	35.0(21)	
90.070	<i>Ginga</i>	0.93	19.2	15.3		36.8	6.75
94.370	BATSE					44(1)	2.3(10)
96.085	<i>RXTE</i>	.855(4)	19.83(11)	10.87(22)	0.80(5)	40.9(5)	4.5(5)
96.562	<i>BeppoSAX</i>				0.73(3)	40.3(2)	6.3(4)
96.567	<i>RXTE</i>	.862(4)	20.23(8)	10.65(15)	0.74(3)	40.8(5)	4.9(3)
96.762	<i>RXTE</i>	.841(5)	19.10(12)	10.02(19)	0.63(3)	39.4(13)	3.8(7)
97.688	<i>RXTE</i>	.901(4)	20.27(9)	10.49(19)	0.66(5)	40.1(7)	4.7(4)
97.860	<i>RXTE</i>	.852(4)	19.50(10)	10.08(16)	0.67(4)	40.0(6)	3.7(6)

[†] Equivalent width (keV) for subtractive Gaussian

Table 4: Average Values of Spectral Parameters in Table 3

	Γ	E_c	E_f	τ	E_r	σ
		keV	keV		keV	keV
Pre-1991	.927(8)	16.52(17)	10.84(20)	0.90(11)	33.67(25)	3.32(34)
Post-1991	.864(10)	19.89(21)	10.40(16)	0.71(3)	41.02(40)	4.83(36)
change	-.063(13)	3.37(27)	-0.44(25)	-.19(11)	7.36(47)	1.51(49)
ratio	.932(13)	1.204(18)	.959(23)	.789(102)	1.218(15)	1.455(184)
χ^2 (no change), dof	210.7/7	281.5/10	35.2/15	47.7/16	831.6/20	35.2/12
χ^2 (change), dof	128.7/5	97.1/8	29.6/13	41.5/14	54.7/18	28.1/10
P_{null}	0.29	0.014	0.33	0.38	$2.3 \cdot 10^{-11}$.33





JD-2440000

